Geomechanics and Engineering, *Vol. 25, No. 4 (2021) 283-294*
DOI: https://doi.org/10.12989/gae.2021.25.4.283

A semi-analytical solution to spherical cavity expansion in unsaturated soils

Jianhua Tang[a], Hui Wang* and Jingpei Li[b]

Department of Civil Engineering, Tongji University, Shanghai 200092, China

(Received December 18, 2020, Revised April 6, 2021, Accepted April 29, 2021)

Abstract. This paper presents a rigorous solution for spherical cavity expansion in unsaturated soils under constant suction condition. The hydraulic behavior that describes the saturation-suction relationship is modeled by a void ratio-dependent soil-water characteristic curve, which allows the hydraulic behavior to fully couple with the mechanical behavior that is described by an extended critical state soil model for unsaturated soil through the specific volume. Considering the boundary condition and introducing an auxiliary coordinate, the problem is formulated to a system of first-order differential equations with three principal stress components and suction as basic unknowns, which is solved as an initial value problem. Parameter analyses are conducted to investigate the effects of suction and the overconsolidation ratio on the overall expansion responses, including the pressure-expansion response, the distribution of the stress components around the cavity, and the stress path of the soil during cavity expansion. The results reveal that the expansion pressures and the distribution of the stress components in unsaturated soils are generally higher than those in saturated soils due to the existence of suction.

Keywords: spherical cavity; suction; hydraulic behaviour; mechanical behavior; expansion responses

1. Introduction

Cavity expansion theory has been widely used in the interpretation of the cone penetration tests (Vesic 1972, Mayne 1991, Salgado *et al.* 1997, Pournaghiazar *et al.* 2012, Diao *et al.* 2015), pressuremeter tests (Carter *et al.* 1986, Cudmani Osinov 2001) and pile installation effects (Randolph 2003, Rezania *et al.* 2017, Wang *et al.* 2020, Liu *et al.* 2020), as these fundamental geotechnical problems can be idealized and simplified as cylindrical or spherical cavity expansion problems with proper assumptions. Recently, the cavity expansion theory is further extended to cavity contraction areas and applied to predict the ground responses induced by tunneling (Hoek 2001, Vrakas and Anagnostou, 2015, Liang *et al.* 2016, Chen *et al.* 2019a, Zou *et al.* 2019, Liang 2020) and the stability of wellbore in engineering (Charlez and Roatesi 1999, Zhang *et al.* 2010, Zhou *et al.* 2021).

Over the past few decades, great research efforts have been devoted to developing new solution techniques and reproducing more realistic soil behavior during cavity expansion. The soil models involved in cavity theory evolve from the early-stage elastic-perfectly models (Carter *et al.* 1986, Yu *et al.* 1991, Lukic *et al.* 2014, Zou *et al.* 2017) to the critical-state models (Collins *et al.* 1992, Silvestri and Abou-Samra 2012, Chen and Abousleiman 2012, 2013, Yang *et al.* 2021a). Recently, more advanced anisotropic soil models and three-dimensional soil models are adopted to model the anisotropic property (Dafalias 1986, Sivasithamparam and Castro 2018, 2020, Li and Zou 2019, Li *et al.* 2021) and three-dimensional strength property (Chen *et al.* 2019b, Yang *et al.* 2020, Li *et al.* 2019) of soils during expansion. However, all the mentioned formulations above are still within the framework of saturated soils, which only have the mechanical response and no change in the degree of saturation during the expansion process. In addition, most soils, especially the clayey ones, are usually unsaturated in the natural state and it is well-known that the mechanical behavior of the unsaturated soil is coupled with hydraulic behavior. Therefore, a rational solution for cavity expansion in unsaturated soil should consider the mutual influences of the hydraulic and mechanical quantities, which makes it quite challenging to derive an analytical solution for the cavity expansion problem. Although several elastoplastic solutions for cavity expansion in unsaturated soil (Russell and Khalili 2006, Yang and Russel 2015) have emerged recently, they can only be regarded as approximate solutions due to the simplification made to mean stress and deviator stress and the ignorance of vertical stress. Besides, the unified bounding surface plasticity model employed only involves one constitutive stress, which is obviously not sufficient for simulating coupled behavior of unsaturated soils.

This paper derives a rigorous solution for drained spherical cavity expansion problem in unsaturated soil. The mechanical response is modeled by the soil model proposed by Sun *et al.* (2008) and the hydraulic response is modeled by a specific volume-dependent soil-water characteristic curve (SWCC), which are coupled subtly through the specific volume. The proposed rigorous solution presents a theoretical basis for the interpretation of in-situ soil tests in

*Corresponding author, Student
E-mail: wanghui97@tongji.edu.cn
[a]Ph.D. Student
E-mail: 1610234@tongji.edu.cn
[b]Professor
E-mail: lijp2773@tongji.edu.cn

ISSN: 2005-307X (Print), 2092-6219 (Online)

unsaturated soils and also presents a generic analytical framework for cavity expansion in unsaturated soils, which can be applied to other coupled hydro-mechanical elastoplastic constitutive models for unsaturated soils, such as the fully coupled models of Wheeler *et al.* (2003), Sheng *et al.* (2008), after a slight modification.

2. Definition of the problem

The first complete formulation of elastoplastic constitutive for unsaturated soil was proposed by Alonso *et al.* (1990). This model, which is later referred to the Barcelona basic model (BBM), remains one of the fundamental and classical models of unsaturated soil. However, the BBM employed the net stress as one of the constitutive stresses while preference is given to the average stress or Bishop stress and suction in recent coupled constitutive models of unsaturated soil as they are more convenient to be implemented in the finite element code and could automatically recover to saturated soil models. Therefore, the coupled hydromechanical model for unsaturated soils developed by Sun *et al.* (2008) is employed in this study to represent the elastoplastic mechanical behavior of the unsaturated soil during cavity expansion. Two constitutive stress components, the average soil skeleton stress tensor σ'_{ij}, also called the Bishop's stress, and the suction s are defined, respectively, as follows

$$\sigma'_{ij} = \sigma_{ij} - [S_{\mathrm{r}}u_{\mathrm{w}} + (1 - S_{\mathrm{r}})u_{\mathrm{a}}]\delta_{ij} \tag{1}$$

$$s = u_{\mathrm{a}} - u_{\mathrm{w}} \tag{2}$$

where u_{a} and u_{w} are the pore-air and pore water pressure, respectively; σ_{ij} is the total stress tensor; S_{r} is the degree of saturation; δ_{ij} is the Kronecker's delta.

In both elastic and plastic regions around the cavity, the equilibrium equation of a given soil particle located at r in the spherical coordinate system as shown in Fig. 1 can be expressed in terms of the total stresses as

$$\frac{\mathrm{d}\sigma_{\mathrm{r}}}{\mathrm{d}r} + 2\frac{\sigma_{\mathrm{r}} - \sigma_{\theta}}{r} \tag{3}$$

where σ_{r} and σ_{θ} are total stress in radial and tangential directions, respectively.

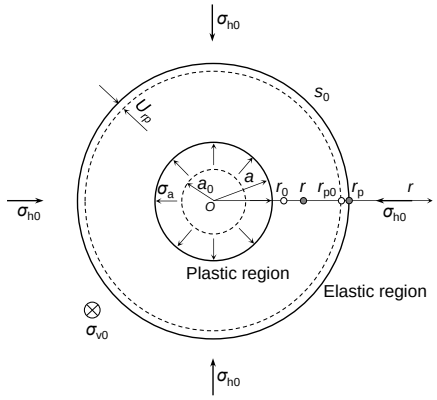

Fig. 1 Schematic representation of a spherical cavity expansion in unsaturated soils

Assuming the pore-air pressure remains constant and equals to the atmospheric pressure p_{at} during the cavity expansion process, the equilibrium equation of an arbitrary material point can be alternatively expressed in terms of the average skeleton stresses as follows:

$$\frac{\mathrm{d}\sigma'_{\mathrm{r}}}{\mathrm{d}r} - S_{\mathrm{r}}\frac{\mathrm{d}s}{\mathrm{d}r} - s\frac{\mathrm{d}S_{\mathrm{r}}}{\mathrm{d}r} + 2\frac{\sigma'_{\mathrm{r}} - \sigma'_{\theta}}{r} \tag{4}$$

where σ'_{r} and σ'_{θ} are average skeleton stress in radial and tangential directions, respectively; and $\mathrm{d}(\ )/\mathrm{d}r$ denotes the differentiation of mechanical quantity with respect to position, which is a Eulerian description.

The SWCC defines the hydraulic behavior of unsaturated soil. The main drying and main wetting curves of the SWCC can be expressed by the incremental form, respectively, as follows (Sun *et al.* 2008)

$$\mathrm{D}S_{\mathrm{r}} = -\lambda_{\mathrm{se}}\mathrm{D}v - \lambda_{\mathrm{sr}}\frac{\mathrm{D}s}{s} \tag{5}$$

$$\mathrm{D}S_{\mathrm{r}} = -\lambda_{\mathrm{se}}\mathrm{D}v - \kappa_{\mathrm{sr}}\frac{\mathrm{D}s}{s} \tag{6}$$

where λ_{se} is the slope of the S_{r}-e curve under constant suction; v is the specific volume; λ_{sr} and κ_{sr} are the slopes of the main drying (or wetting) curve and the scanning curve, respectively; $\mathrm{D}(\ )$ denotes the differentiation of mechanical quantity of a given soil particle which is a Lagrangian description.

The LC yield function along with the associated flow rule defines the mechanical behavior of unsaturated soil, which is given by

$$f = q^2 + M^2 p'(p' - p'_{\mathrm{y}}) \tag{7}$$

where M is the slope of the critical state line in $p' - q$ plane; $p' = \sigma'_{ij}\delta_{ij}/3$ is the mean stress; $q = \sqrt{3s_{ij}s_{ij}/2}$ is the deviatoric stress; $s_{ij} = \sigma'_{ij} - p'\delta_{ij}$ is the deviatoric stress tensor; p'_{y} is the yield stress for unsaturated soil with suction s, which can be related to the yield stress for saturated soil $p'_{0\mathrm{y}}$ as

$$p'_{\mathrm{y}} = p'_{\mathrm{n}}\left(\frac{p'_{0\mathrm{y}}}{p'_{\mathrm{n}}}\right)^{\frac{\lambda(0)-\kappa}{\lambda(s)-\kappa}} \tag{8}$$

in which p'_{n} is a reference stress; κ is the slope of unloading line for unsaturated soil; $\lambda(0)$ and $\lambda(\mathrm{s})$ are the slopes of the normal compression lines of saturated soil and unsaturated soil with suction s in the $e - \ln p'$ plane. The $\lambda(\mathrm{s})$ can be related to $\lambda(0)$ as follows Alonso *et al.* (1990)

$$\lambda(s) = \lambda(0)[(1 - b)e^{-cs} + b] \tag{9}$$

where e is the void ratio; b and c are two material parameters.

According to the associated flow rule, the plastic strain increment tensor $\mathrm{D}\varepsilon^{\mathrm{p}}_{ij}$ induced by loading can be determined from the LC yield function as

$$\mathrm{D}\varepsilon^{\mathrm{p}}_{ij} = \Lambda\frac{\partial f}{\partial \sigma'_{ij}} \tag{10}$$

The scalar multiplier Λ can be determined from the

plastic consistency condition as shown in Appendix.

3. Elastic analysis

The stress distributions and the radial displacement of an arbitrary soil particle in the elastic region can be easily given as (Yang *et al.* 2021b)

$$\sigma_{\mathrm{r}}' = p_0' + (p_{\mathrm{p}}' - p_0')\left(\frac{r_{\mathrm{p}}}{r}\right)^3 \tag{11}$$

$$\sigma_{\theta}' = p_0' - \frac{1}{2}(p_{\mathrm{p}}' - p_0')\left(\frac{r_{\mathrm{p}}}{r}\right)^3 \tag{12}$$

$$U_{\mathrm{r}} = \frac{(1+\mu)\left(\sigma_{\mathrm{rp}}' - \sigma_{\mathrm{h0}}'\right)}{2E}\left(\frac{r_{\mathrm{p}}}{r}\right)^3 \tag{13}$$

where σ_{rp}', r_{p} and p_{p}' are the radial average skeleton stress, the radius of the plastic region and mean stress at the elastic-plastic boundary, respectively; p_0' is the in situ mean stress; σ_{h0}' is the in situ horizontal average skeleton stress; E denotes elastic modulus, which can be expressed as a function of the mean stress p' and the specific volume v as

$$E = \frac{3(1-2\mu)vp'}{\kappa} \tag{14}$$

where μ denotes Poisson's ratio.

The suction keeps unchanged in the elastic region, which gives

$$s = s_0 \tag{15}$$

where s_0 is the in situ suction. The volumetric strain increment $\mathrm{D}\varepsilon_{\mathrm{v}}$ vanishes everywhere in the elastic region, i.e.,

$$\mathrm{D}\varepsilon_{\mathrm{v}} = \frac{3(1-2\mu)}{E}\mathrm{D}p' \tag{16}$$

On the other hand, the volumetric strain increment can be expressed by the specific volume by

$$\mathrm{D}\varepsilon_{\mathrm{v}} = -\frac{\mathrm{D}v}{v} \tag{17}$$

Combining Eqs. (5), (6), (16) and (17), the degree of saturation can be given as

$$S_{\mathrm{r}} = S_{\mathrm{r0}} \tag{18}$$

(18)

where S_{r0} is the initial value of degree of saturation.

4. Plastic analysis

The total principal strain increments, $\mathrm{D}\varepsilon_{\mathrm{r}}$ and $\mathrm{D}\varepsilon_{\theta}$ of an arbitrary material particle in the plastic region can be decomposed into elastic component and plastic component as

$$\mathrm{D}\varepsilon_{\mathrm{r}} = \mathrm{D}\varepsilon_{\mathrm{r}}^{\mathrm{e}} + \mathrm{D}\varepsilon_{\mathrm{r}}^{\mathrm{p}} \tag{19}$$

$$\mathrm{D}\varepsilon_{\theta} = \mathrm{D}\varepsilon_{\theta}^{\mathrm{e}} + \mathrm{D}\varepsilon_{\theta}^{\mathrm{p}} \tag{20}$$

where $\mathrm{D}\varepsilon_{\mathrm{r}}^{\mathrm{e}}$ and $\mathrm{D}\varepsilon_{\theta}^{\mathrm{e}}$ denote the two principle elastic strain increments in radial and circumferential directions, which can be easily calculated by Hooke's law; $\mathrm{D}\varepsilon_{\mathrm{r}}^{\mathrm{p}}$ and $\mathrm{D}\varepsilon_{\theta}^{\mathrm{p}}$ are the two principal plastic strain increments in radial and circumferential directions.

Based on the associated flow rule given by Eq. (10) and the yield function of Eq. (7), the principal plastic strain increments can be expressed as

$$\mathrm{D}\varepsilon_{\mathrm{r}}^{\mathrm{p}} = AA_{\mathrm{r}}(A_{\mathrm{r}}\mathrm{D}\sigma_{\mathrm{r}}' + 2A_{\theta}\mathrm{D}\sigma_{\theta}' + A_{\mathrm{s}}\mathrm{D}s) \tag{21}$$

$$\mathrm{D}\varepsilon_{\theta}^{\mathrm{p}} = AA_{\theta}(A_{\mathrm{r}}\mathrm{D}\sigma_{\mathrm{r}}' + 2A_{\theta}\mathrm{D}\sigma_{\theta}' + A_{\mathrm{s}}\mathrm{D}s) \tag{22}$$

where

$$A = \frac{\lambda(S)-\kappa}{M^2 p'^2 p_{0\mathrm{y}}' v(M^2-\eta^2)}\left(\frac{p_{0\mathrm{y}}'}{p_{\mathrm{n}}'}\right)^{-\frac{\lambda(0)-\lambda(s)}{\lambda(s)-\kappa}} \tag{23}$$

$$A_{\mathrm{r}} = \frac{1}{3}(M^2-\eta^2)p' + 3(\sigma_{\mathrm{r}}' - p') \tag{24}$$

$$A_{\theta} = \frac{1}{3}(M^2-\eta^2)p' + 3(\sigma_{\theta}' - p') \tag{25}$$

$$A_{\mathrm{s}} = \frac{p'^2(M^2+\eta^2)\lambda(0)[\lambda(0)-\kappa]c(1-b)e^{-cs}}{[\lambda(s)-\kappa]^2}\ln\left(\frac{p_{\mathrm{n}}'}{p_{0\mathrm{y}}'}\right) \tag{26}$$

$$\eta = \frac{q}{p'} \tag{27}$$

From Eqs. (7)-(9), $p_{0\mathrm{y}}'$ can be expressed as a function of the current stress state as

$$p_{0\mathrm{y}}' = p_{\mathrm{n}}'\left(\frac{M^2+\eta^2}{M^2}\frac{p'}{p_{\mathrm{n}}'}\right)^{\frac{\lambda(0)[(1-b)e^{-cs}+b]-\kappa}{\lambda(0)-\kappa}} \tag{28}$$

For the spherical cavity expansion problems, the strain increment components and stress increment components can be related to each other, which would simplify the problem and provide the essential conditions to get an analytical solution for the problem considered. The constitutive matrix for spherical cavity expansion problem can be given as follows

$$\begin{bmatrix}\mathrm{D}\sigma_{\mathrm{r}}' \\ \mathrm{D}\sigma_{\theta}' \\ \mathrm{D}s\end{bmatrix} = \begin{bmatrix}B_{11}/\Delta & B_{12}/\Delta & B_{13}/\Delta_1 \\ B_{21}/\Delta & B_{22}/\Delta & B_{23}/\Delta_1 \\ 0 & 0 & B_{33}\end{bmatrix}\begin{bmatrix}\mathrm{D}\varepsilon_{\mathrm{r}} \\ \mathrm{D}\varepsilon_{\theta} \\ \mathrm{D}S_{\mathrm{r}} + \lambda_{\mathrm{se}}\mathrm{D}v\end{bmatrix} \tag{29}$$

where

$$B_{11} = E(2EAA_{\theta}^2 + 1 - \mu) \tag{30}$$

$$B_{12} = 2E(\mu - EAA_{\mathrm{r}}A_{\theta}) \tag{31}$$

$$B_{13} = AA_{\mathrm{s}}E[(1-\mu)A_{\mathrm{r}} + 2\mu A_{\theta}] \tag{32}$$

$$B_{22} = E(EAA_{\mathrm{r}}^2 + 1) \tag{33}$$

$$B_{23} = EAA_{\mathrm{s}}(A_{\theta} + \mu A_{\mathrm{r}}) \tag{34}$$

$$B_{33} = -\frac{s}{\beta} \tag{35}$$

$$\Delta = EA\left(A_{\mathrm{r}}^2 - \mu A_{\mathrm{r}}^2 + 4\mu A_{\mathrm{r}}A_{\theta} + 2A_{\theta}^2\right) + 1 - \mu - 2\mu^2 \tag{36}$$

$$\Delta_1 = \frac{\beta}{s}\left[EA\left(A_{\mathrm{r}}^2 - \mu A_{\mathrm{r}}^2 + 2A_{\theta}^2 + 4\mu A_{\mathrm{r}}A_{\theta}\right) + 1 - \mu - 2\mu^2\right] \tag{37}$$

To make constitutive matrix solvable, the strain increments can be related to the specific volume through an auxiliary variable $\xi(=U_{\mathrm{r}}/r)$ proposed by Chen and Abousleiman (2013) as follows

$$\mathrm{D}\varepsilon_{\theta} = -\frac{\mathrm{D}\xi}{1-\xi} \tag{38}$$

$$\mathrm{D}\varepsilon_{\mathrm{r}} = \mathrm{D}\varepsilon_{\mathrm{v}} - 2\mathrm{D}\varepsilon_{\theta} = -\frac{\mathrm{D}v}{v} + \frac{2\mathrm{D}\xi}{1-\xi} \tag{39}$$

The drained condition for unsaturated soils means the suction s of soil keeps constant during loading, which usually corresponds to an extremely slow cone penetration test or pressuremeter test. The constant suction condition can be mathematically expressed as

$$\mathrm{D}s = 0 \tag{40}$$

Since the suction keeps as a constant in the cavity expansion process, the mechanical and hydraulic responses can be decoupled and considered separately for the problem considered. Hence, the mechanical responses can be determined solely from the mechanical components, and the hydraulic responses can then be determined by the specific volume calculated from the mechanical components. Based on Eq. (29), the decoupled constitutive matrix for the mechanical behavior of the soil around the cavity can be written as

$$\begin{bmatrix}\mathrm{D}\sigma_{\mathrm{r}}' \\ \mathrm{D}\sigma_{\theta}'\end{bmatrix} = \begin{bmatrix}B_{11}/\Delta & B_{12}/\Delta \\ B_{21}/\Delta & B_{22}/\Delta\end{bmatrix}\begin{bmatrix}\mathrm{D}\varepsilon_{\mathrm{r}} \\ \mathrm{D}\varepsilon_{\theta}\end{bmatrix} \tag{41}$$

Note that the form of the constitutive matrix above is similar to that for drained expansion of a spherical cavity presented by Li *et al.* (2017), but it contains the effects of suction, since the B_{ij} and Δ are explicit functions of suction s, the two stress variables $\sigma_{\mathrm{r}}', \sigma_{\theta}'$ and the specific volume v. To fully formulate the problem, it also needs to make use of the equilibrium equation as there are essentially three basic unknown variables $\sigma_{\mathrm{r}}', \sigma_{\theta}'$ and v in Eq. (41). Due to radial position r is related to auxiliary variable ξ, the equilibrium equation Eq. (4), under constant suction condition, can be written as

$$\frac{\mathrm{D}\sigma_{\mathrm{r}}'}{\mathrm{D}\xi}\frac{\mathrm{d}\xi}{\mathrm{d}r} + s\lambda_{\mathrm{se}}\frac{\mathrm{D}v}{\mathrm{D}\xi}\frac{\mathrm{d}\xi}{\mathrm{d}r} + \frac{2(\sigma_{\mathrm{r}}' - \sigma_{\theta}')}{r} = 0 \tag{42}$$

Following the similar procedure of Chen and Abousleiman (2013), the derivative of auxiliary variable ξ with respect to radial position r can be expressed as

$$\frac{\mathrm{d}\xi}{\mathrm{d}r} = -\frac{U_{\mathrm{r}}}{r^2} + \frac{1}{r}\frac{\mathrm{d}U_{\mathrm{r}}}{\mathrm{d}r} = \frac{1}{r}\left\{1 - \left[\frac{v}{v_0}(1-\xi)\right]^{-2} - \xi\right\} \tag{43}$$

Substituting Eq. (43) into Eq. (42), the equilibrium equation can be transformed from Eulerian description to Lagrangian description as

$$\left(\frac{\mathrm{D}\sigma_{\mathrm{r}}'}{\mathrm{D}\xi} + s\lambda_{\mathrm{se}}\frac{\mathrm{D}v}{\mathrm{D}\xi}\right)\frac{1}{r}\left\{1 - \left[\frac{v}{v_0}(1-\xi)\right]^{-2} - \xi\right\} + \frac{2(\sigma_{\mathrm{r}}' - \sigma_{\theta}')}{r} = 0 \tag{44}$$

Now, the problem of drained expansion of a spherical cavity in unsaturated soils can be finally formulated as a system of three first-order differential equations by combining Eqs. (41) and (44) as

$$\frac{\mathrm{D}v}{\mathrm{D}\xi} = \left[\frac{2(\sigma_{\mathrm{r}}' - \sigma_{\theta}')}{1 - v_0/v/(1-\xi)^2 - \xi} + \frac{B_{12} - 2B_{11}}{\Delta(\xi - 1)}\right]\frac{\Delta v}{B_{11} - s\lambda_{\mathrm{se}}\Delta v} \tag{45}$$

$$\frac{\mathrm{D}\sigma_{\mathrm{r}}'}{\mathrm{D}\xi} = -\frac{B_{11}}{\Delta v}\frac{\mathrm{D}v}{\mathrm{D}\xi} + \frac{B_{12} - 2B_{11}}{\Delta(\xi - 1)} \tag{46}$$

$$\frac{\mathrm{D}\sigma_{\theta}'}{\mathrm{D}\xi} = -\frac{B_{21}}{\Delta v}\frac{\mathrm{D}v}{\mathrm{D}\xi} + \frac{B_{22} - 2B_{21}}{\Delta(\xi - 1)} \tag{47}$$

The above governing differential equations are valid for any material point currently in the annulus plastic area $a \le r \le r_{\mathrm{p}}$ and can be readily solved as an initial value problem if the initial values of the basic variables are known. After obtaining the specific volume from Eq. (45), the degree of saturation S_{r} in the plastic region can be easily determined from Eq. (5). Integrating Eq. (5) with attention of $\mathrm{d}s = 0$ gives

$$S_{\mathrm{r}} = S_{\mathrm{rp}} - \lambda_{\mathrm{se}}(v - v_0) \tag{48}$$

where S_{rp} denotes the degree of saturation at the elastic-plastic boundary.

5. Initial conditions

The initial conditions of the investigated problem should be the values of basic variables at the elastic-plastic boundary, which should satisfy both the solutions to elastic region and plastic region. Hence, the specific volume v_{p}, the suction s_{p} and the degree of saturation S_{rp} at elastic-plastic boundary can be easily given, respectively, as

$$v_{\mathrm{p}} = v_0 \tag{49}$$

$$s_{\mathrm{p}} = s_0 \tag{50}$$

$$S_{\mathrm{rp}} = S_{\mathrm{r0}} \tag{51}$$

where v_0 is the initial value of specific volume. The value of two stress components at elastic-plastic boundary can be determined according to the continuity condition at the elastic-plastic boundary as follows

$$\sigma_{\mathrm{rp}}' = \sigma_{\mathrm{h0}}' + \frac{2}{3}q_{\mathrm{p}} \tag{52}$$

$$\sigma_{\theta\mathrm{p}}' = \sigma_{\mathrm{h0}}' - \tfrac{1}{3}q_{\mathrm{p}} \tag{53}$$

where q_{p} is the deviatoric stress of the material particle that yields, which can be associated with the

overconsolidation ratio, R_{us} as

$$q_p = Mp_0'\sqrt{R_{us}-1} \tag{54}$$

The initial condition of the auxiliary variable, ξ_p, can be obtained as

$$\xi_p = \left(\frac{U_r}{r}\right)_{r=r_p} = \frac{(\sigma_{rp}-\sigma_{h0})(1+\mu)}{2E} \tag{55}$$

Up to now, all the values of the basic unknowns at elastic-plastic boundary have been already determined. However, it should be noted that all the results are now expressed as functions of the auxiliary variable ξ rather than the original position r. Hence, the relationship between the radial coordinate r and the auxiliary variable ξ can be transformed as

$$\frac{r}{a} = \exp\left(\int_{\xi_a}^{\xi} \frac{v(1-\xi)^2}{v(1-\xi)^3 - v_0} d\xi\right) \tag{56}$$

where $\xi_a = 1 - a/a_0$ is the auxiliary variable at the cavity wall and $\xi_a > \xi > \xi_p$.

6. Results and discussions

In this part, the proposed solution is first validated by comparing the cavity expansion responses with those from the rigorous solution of Li *et al.* (2017) developed for fully drained expansion of a spherical cavity in saturated soils. Subsequently, the results, including the distributions of the mechanical and hydraulic parameters, the expansion response curves as well as the stress paths of a typical element at the cavity wall, will be shown. Also, those results with suction to be zero are included to investigate the effects of coupled hydromechanical behavior on the cavity expansion process. The parameters used in the parametric study are summarized in Table 1, which were first summarized and extended by Chen *et al.* (2020) from Alonso *et al.* (1990) and Sun *et al.* (2008) to give the results with the best performance.

6.1 Validation

To validate the proposed solution, zero suction is applied to the proposed solution and zero hydrostatic water pressure is applied to the solution of Li *et al.* (2017). Figs. 2(a)-2(c) compare the stress trajectory of a soil particle at the cavity wall during cavity expansion, the distributions of the stress components and specific volume at the instance $a/a_0 = 2$ as well as the expansion-pressure curves generated from the proposed solution with those from the rigorous solution of Li *et al.* (2017) without considering the hydrostatic water pressure. Note that the proposed drained solution become identical to the results of Li *et al.* (2017)

Table 1 Soil parameters adopted for different cases used in analysis

R_{us}	σ_{h0}: kPa	σ_{v0}: kPa	p_0: kPa	q_0: kPa	K_0	p'_a: kPa	p'_{y0}: kPa	p_{0y}: kPa
1	120	120	120	0	1	132	132	46.8
1.2	120	120	120	0	1	132	158.4	52.2
3	120	120	120	0	1	132	396	90.4
5	120	120	120	0	1	132	660	122.7

M=1.2, c = 0.65, b = 0.125, $\lambda(0)$ = 0.15, λ_{se} = 0.21, k = 0.6, p_{at} = 100 kPa, κ_s = 0.008, β = 0.12, v_0 = 2.1, κ = 0.03, μ = 0.3, p'_n = 10 kPa, s_0 = 100 kPa, S_{r0} = 0.6, w_0 = 24.09%, G_s = 2.74

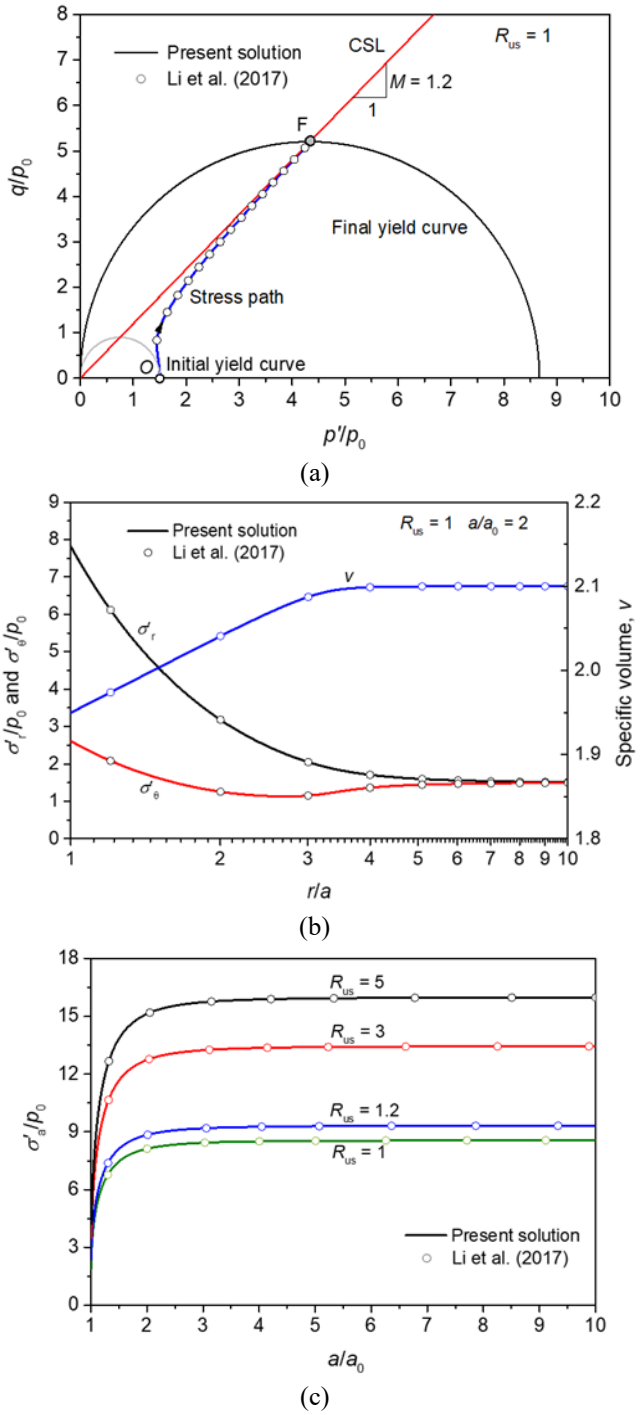

Fig. 2 Comparisons of (a) stress trajectory in $p'-q$ plane, (b) distributions of stress components and specific volume and (c) expansion-pressure curves with solution without considering suction

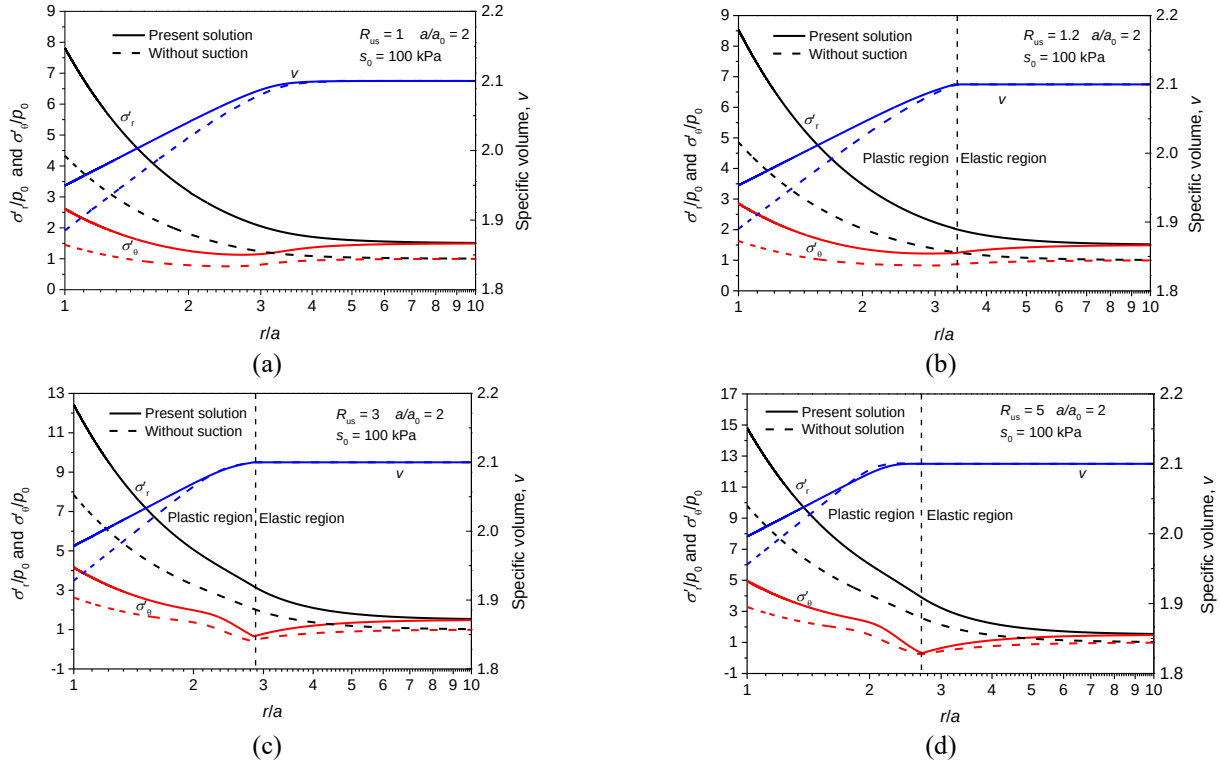

Fig. 3 Distributions of normalized stress components and specific volume around cavity: (a) $R_{\mathrm{us}} = 1$, (b) $R_{\mathrm{us}} = 1.2$, (c) $R_{\mathrm{us}} = 3$ and (d) $R_{\mathrm{us}} = 5$

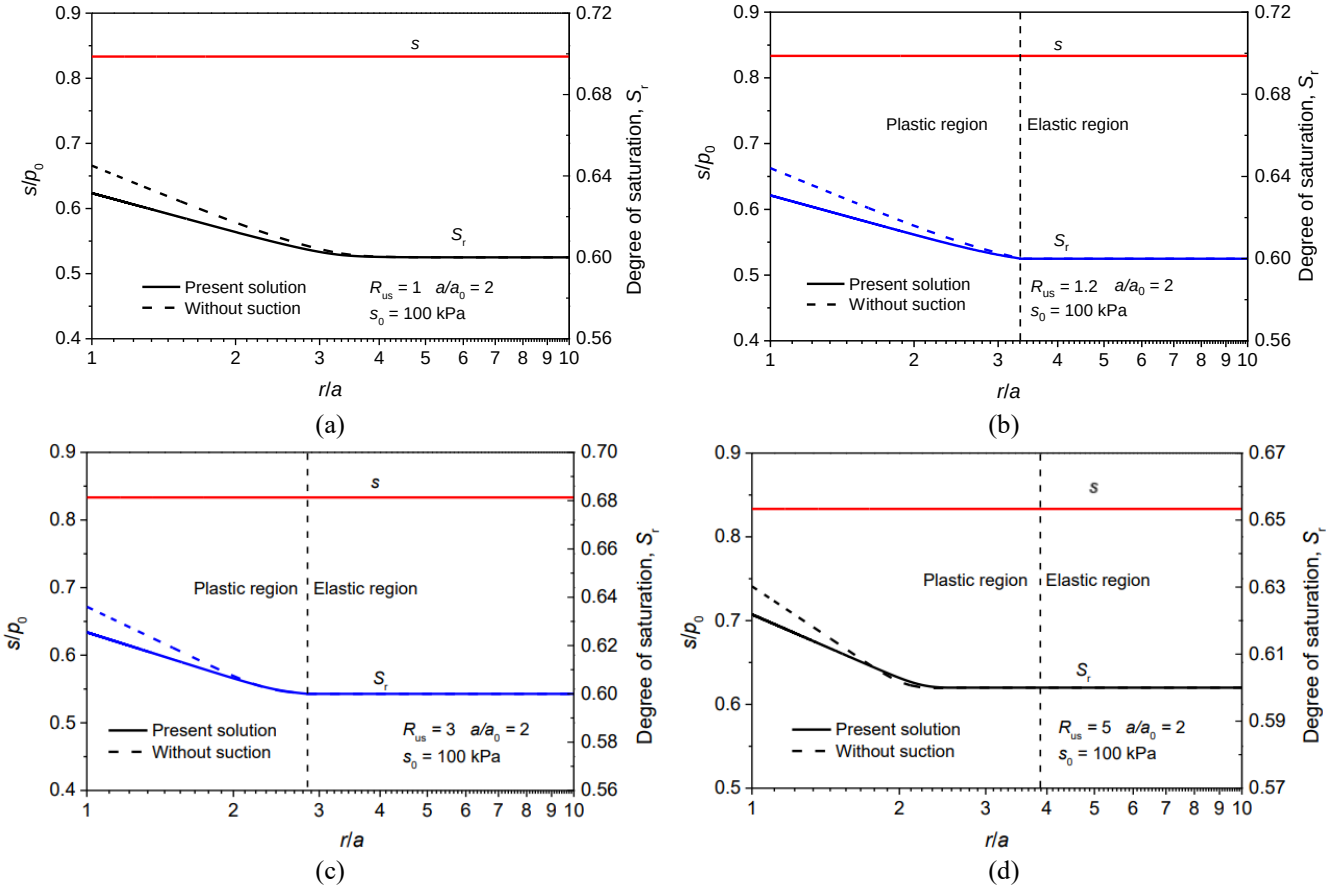

Fig. 4 Distributions of normalized suction and degree of saturation around cavity: (a) $R_{\mathrm{us}} = 1$, (b) $R_{\mathrm{us}} = 1.2$, (c) $R_{\mathrm{us}} = 3$ and (d) $R_{\mathrm{us}} = 5$

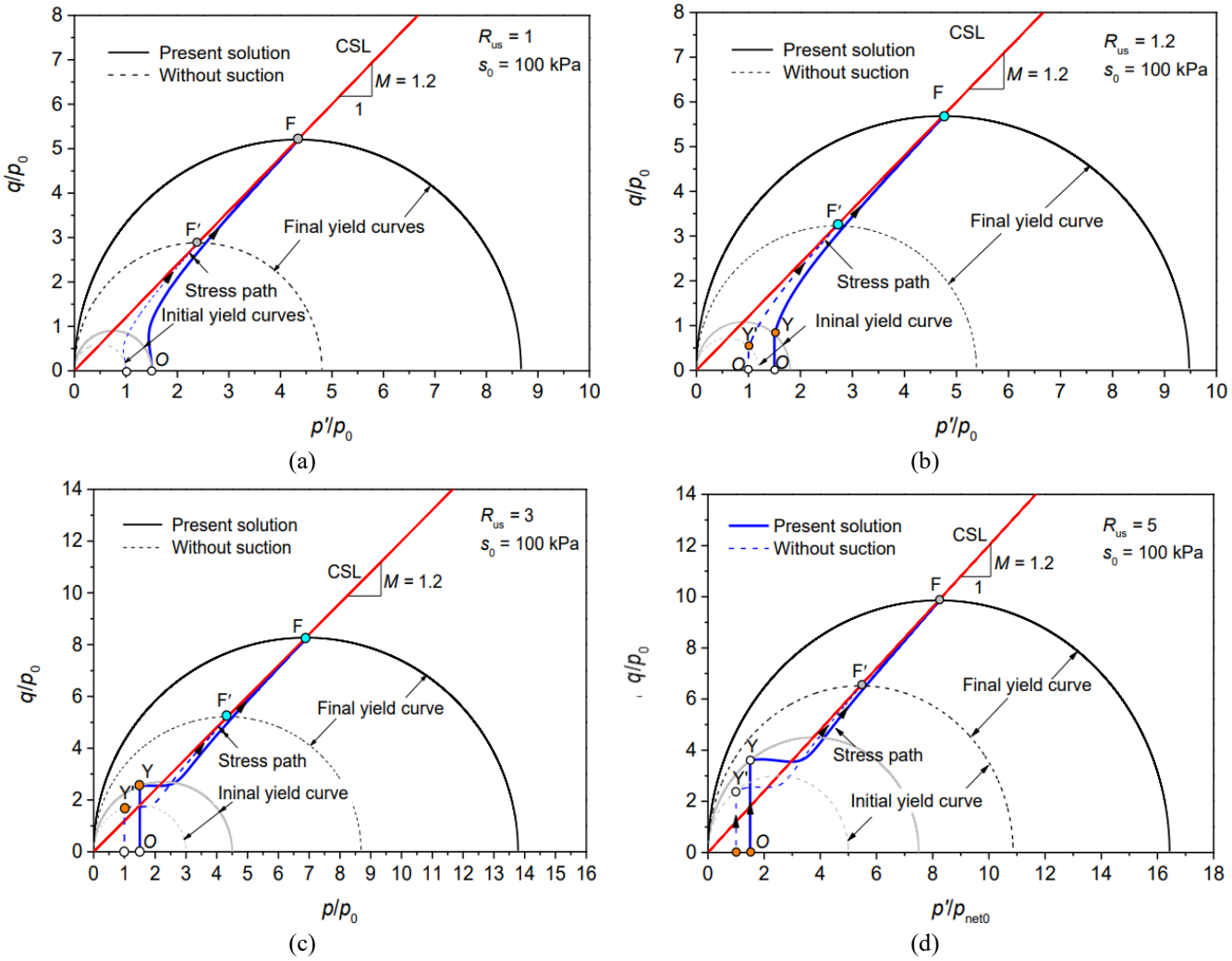

Fig. 5 Stress paths of a soil particle at cavity wall in $p' - q$ plane: (a) $R_{\mathrm{us}} = 1$, (b) $R_{\mathrm{us}} = 1.2$, (c) $R_{\mathrm{us}} = 3$ and (d) $R_{\mathrm{us}} = 5$

when suction approaches zero. It can be seen from Figs. 2(a)-2(c) that the proposed solution perfectly reduces to the rigorous solution of Li *et al.* (2017) when the suction equals to zero, which sufficiently demonstrates the validity of the proposed solution for the drained case.

6.2 Distributions of mechanical and hydraulic parameters

Figs. 3(a)-3(d) show the distributions of the radial and tangential stresses $\sigma_{\mathrm{r}}', \sigma_{\theta}'$, and the specific volume v around the cavity with different values of R_{us} when the expansion ratio a/a_0 equals to 2. All the stress parameters in Fig. 3 are normalized by dividing the initial mean stress p_0 and the radial location r is normalized by the initial cavity radius a_0, so do the other figures. Also the results with zero suction, included in those figures, are presented to investigate the effects of suction on the expansion responses. Although the distributions of the stress and specific volume around the cavity in unsaturated soils show similar patterns to those without suction, it can be observed that the principal stresses predicted by the present solution are higher than those without suction, which indicates that suction exerts permanent enhancement on the strength and stiffness of the unsaturated soils during cavity expansion. It is also not hard to find that the magnitude of stress components at the cavity wall increases with R_{us}, but the specific volume is insensitive to R_{us}. Moreover, the discrepancy between the results with and without suction is narrowed to a certain degree as R_{us} increases.

Fig. 4 plots the distributions of the hydraulic parameters (i.e., the normalized suction s/p_0 and the degree of saturation S_{r}) around the cavity with different R_{us} when the expansion ratio a/a_0 is equal to 2. It is understandable that the suction maintains constant around the cavity for all cases, while the degree of saturation of the soil near the cavity is larger than soil at infinity. In addition, the degree of saturation changes less significantly in soil with suction. This can be well explained by Eq. (5) that the degree of saturation depends on the specific volume and the reciprocal of suction. However, the overconsolidation ratio seems to have a very limited effect on the distribution of the degree of saturation under drained conditions. This is because the change of the degree of saturation primarily depends on the change of the specific volume under drained condition, which is insensitive to the overconsolidation ratio

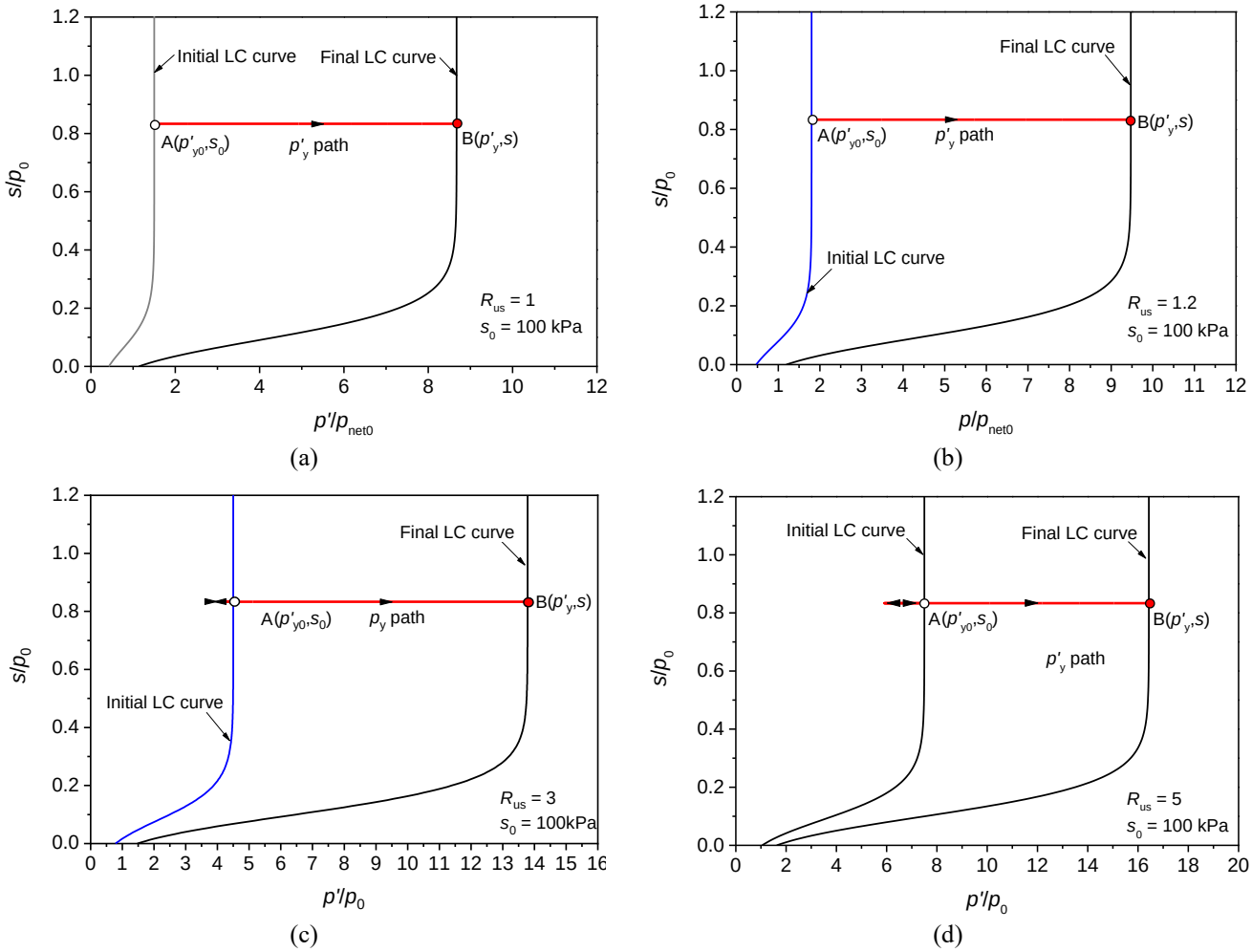

Fig. 6 p'_{y} paths and projections of skeleton stress path in $p'-\mathrm{s}$ plane: (a) $R_{\mathrm{us}}=1$, (b) $R_{\mathrm{us}}=1.2$, (c) $R_{\mathrm{us}}=3$ and (d) $R_{\mathrm{us}}=5$

and barely changes under the drained condition with high suction.

6.3 Stress paths

To investigate the development of the stress state of a soil element and the evolution of the yield surface during the expansion process, Figs. 5 and 6 depict the stress paths of a typical soil element at the cavity wall and the evolutions of the yield surface for cases with different $\mathrm{R_{us}}$ in $p'-q$ plane and $p'-s$ plane, respectively. In those figures, points O, Y, and F denote the original, yield and final state of the investigated soil particle and those with prime mean the hydromechanical state of the solution without suction. For $R_{\mathrm{us}}=1$, the stress path moves directly to the critical state line (CSL) and terminates at point F. For other OCRs, the stress paths move vertically to the initial yield surface at first and then turn up and right to the critical state line. It is noteworthy that the stress paths of moderately consolidated soil ($R_{\mathrm{us}}=3{,}5$) seem to have crossed the CSL. This phenomenon indicates that the moderately consolidated soil shrinks at first and then dilates.

Since the suction keeps unchanged for the drained case, the projections of stress trajectories and the p'_{y} paths are horizontal straight lines and some portion of the projection overlaps the p'_{y} path in $p'-\mathrm{s}$ plane. For clarity, the projections of skeleton stress trajectories are therefore not plotted in Fig. 6. It can be observed from Fig. 6 that apart from the p'_{y} path for $R_{\mathrm{us}}=3{,}5$, all the p'_{y} paths move horizontally from point $\mathrm{O}(p'_{\mathrm{y0}},s_0)$ towards point $F(p'_{\mathrm{yf}},s_{\mathrm{f}})$ as the suction keeps unchanged during the drained expansion processes. However, the $\mathrm{p'_y}$ path for moderately consolidated soils ($R_{\mathrm{us}}=3{,}5$) firstly move horizontally left after yielding and then turn right towards point $\mathrm{B}(p'_{\mathrm{y}},\mathrm{s})$. The above observations again indicate that the LC yield surfaces of the normally consolidated and slightly overconsolidated soils expand while the LC yield surfaces of the moderately consolidated soils contract then expand in the three dimensional p'-q-s stress space during the drained expansion processes.

6.4 Expansion process

The normalized expanding pressure $\sigma_{\mathrm{a}}/p_{0,}$ the degree of saturation S_{r} for a soil element at the cavity wall as well as the normalized elastic-plastic radius r_{p}/a are plotted

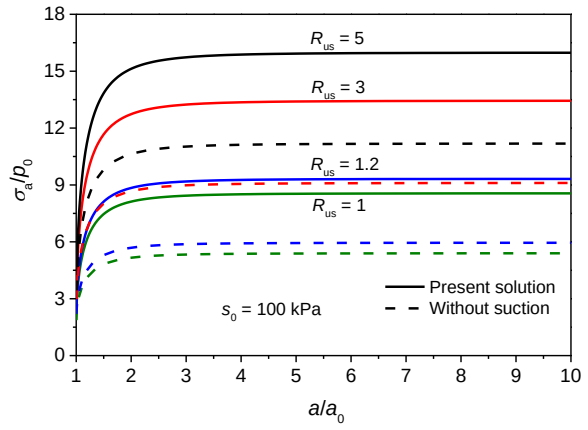

Fig. 7 Variations of the expanding pressure with normalized cavity radius

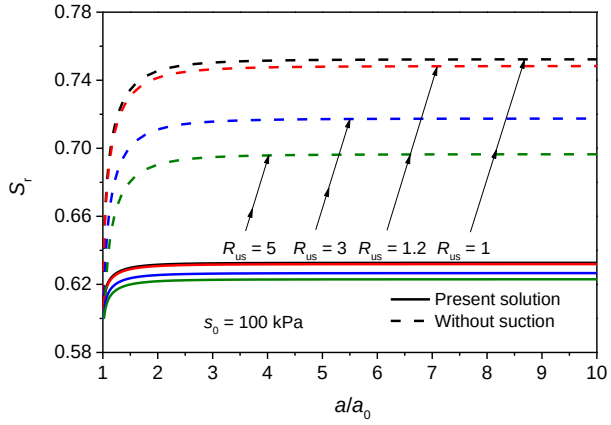

Fig. 8 Variations of degree of saturation at cavity wall with normalized cavity radius

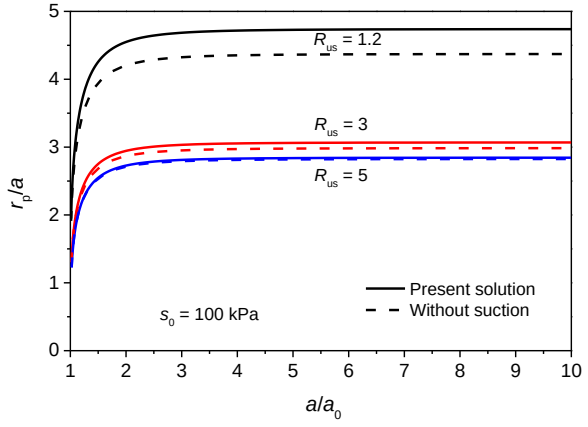

Fig. 9 Variations of the expanding pressure with normalized cavity radius

against the normalized cavity radius a/a_0 for cases with different R_{us} in Fig. 7, Fig. 8, and Fig. 9, respectively. As shown in the three figures, all the expansion curves increase dramatically at the initial stage of expansion ($a/a_0 < 2$), and then gradually approach to constant values. As overconsolidation ratio increases, the expanding pressure increases significantly. Therefore, a larger plastic zone is formed around the cavity. However, the overconsolidation ratio appears to have minor impacts on the degree of saturation of unsaturated soils due to the existence of suction as explained in Eq. (5). For comparison, the results without suction are also included to explore the coupled hydromechanical effects on the expansion response. It is clearly shown that the expanding pressure and the radius of the elastic-plastic boundary are smaller for soils without suction since the suction stress acts as an enhancement to soil structure. As a contrast, the degree of saturation varies significantly with the overconsolidation ratio in soils without suction, which illustrates the predominant difference between the unsaturated soils and saturated soils.

7. Conclusions

This paper presents a rigorous semi-analytical solution to drained spherical cavity expansion in unsaturated soils. The mechanical behavior and hydraulic behavior are modeled by the unsaturated soil model proposed by Sun *et al.* (2008) and coupled through the specific volume. By taking advantage of the stress-strain relationship and the SWCC, the elastoplastic constitutive matrix, and the governing equation for the problem considered is developed. With the aid of an auxiliary variable, the governing equation can be readily solved as an initial value problem. Special attention is paid to investigate the impacts of suction and coupled hydromechanical behavior on the expansion response in the parametric study. Results show that the suction enhances the stiffness and strength of the unsaturated soils and consequently results in a larger expanding pressure for expansion and a larger plastic region. The proposed solution constitutes a theoretical basis for rigorous modeling of the cavity expansion problems in unsaturated soils and can be used to interpret the pressuremeter tests and pile installation effects in unsaturated soils.

References

Alonso, E.E., Gens, A. and Josa, A. (1990), "A constitutive model for partially saturated soils", *Géotechnique*, **40**(3), 405-430. https://doi.org/10.1680/geot.1990.40.3.405.

Carter, J.P., Booker, J.R. and Yeung, S.K. (1986), "Cavity expansion in cohesive frictional soils", *Géotechnique,* **36**(3), 349-358. https://doi.org/10.1680/geot.1986.36.3.349.

Charlez, P.A. and Roatesi, S. (1999), "A fully analytical solution of the wellbore stability problem under undrained conditions using a linearized Cam-Clay model", *Oil Gas Sci. Technol.*, **54**(5), 551-563. https://doi.org/10.2516/ogst:1999047.

Chen, G.H., Zou, J.F. and Qian, Z.H. (2019a). "An improved collapse analysis mechanism for the face stability of shield tunnel in layered soils", *Geomech. Eng.*, **17**(1), 97-107. https://doi.org/10.12989/gae.2019.17.1.097.

Chen, H.H., Li, L. and Li, J.P. (2019b), "Stress transform method to undrained and drained expansion of a cylindrical cavity in anisotropic modified cam-clay soils", *Comput. Geotech.*, **106**, 128-142. https://doi.org/10.1016/j.compgeo.2018.10.016.

Chen, H.H., Li, L., Li, J.P. and Sun, D.A. (2020), "Elastoplastic solutions for cylindrical cavity expansion in unsaturated soils", *Comput. Geotech.*, **123**, 103569. https://doi.org/10.1016/j.compgeo.2020.103569.

Chen, S.L. and Abousleiman, Y.N. (2012), "Exact undrained elasto-plastic solution for cylindrical cavity expansion in modified Cam Clay soil", *Géotechnique*, **62**(5), 447-456. https://doi.org/10.1680/geot.11.P.027.

Chen, S.L. and Abousleiman, Y.N. (2013). "Exact drained solution for cylindrical cavity expansion in modified Cam Clay soil", *Géotechnique*, **63**(6), 510-517. https://doi.org/10.1680/geot.11.P.088.

Collins, I.F., Pender, M.J. and Wang, Y. (1992), "Cavity expansion in sands under drained loading conditions", *Int. J. Numer. Anal. Met.*, **16**(1), 3-23. https://doi.org/10.1002/nag.1610160103.

Cudmani, R. and Osinov, V.A. (2001), "The cavity expansion problem for the interpretation of cone penetration and pressuremeter tests", *Can. Geotech. J.*, **38**(3), 622-638. https://doi.org/10.1139/cgj-38-3-622.

Dafalias, Y.F. (1986), "An anisotropic critical state soil plasticity model", *Mech. Res. Commun.*, **13**(6), 341-347. https://doi.org/10.1016/0093-6413(86)90047-9.

Diao, H.J., Wu, Y.D., Liu, J. and Luo, R.P. (2015), "An analytical investigation of soil disturbance due to sampling penetration", *Geomech. Eng.*, **9**(6), 743-755. https://doi.org/10.12989/gae.2015.9.6.743.

Hoek, E. (2001), "Big tunnels in bad rock", *J. Geotech. Geoenviron. Eng.*, **127**(9), 726-740. https://doi.org/10.1061/(ASCE)1090-0241(2001)127:9(726).

Li, C. and Zou, J.F. (2019), "Created cavity expansion solution in anisotropic and drained condition based on Cam-clay model", *Geomech. Eng.*, **19**(2), 141-151. https://doi.org/10.12989/gae.2019.19.2.141.

Li, C., Zou, J.F. and Sheng Y.M. (2020), "Undrained solution for cavity expansion in strength degradation and tresca soils", *Geomech. Eng.*, **21**(6), 527-536. https://doi.org/10.12989/gae.2020.21.6.527.

Li, L., Chen, H.H., Li, J.P. and Sun, D.A. (2021), "An elastoplastic solution to undrained expansion of a cylindrical cavity in SANICLAY under plane stress condition", *Comput. Geotech.*, **132**, 103990. https://doi.org/10.1016/j.compgeo.2020.103990.

Li, L., Li, J.P., Sun, D.A. and Gong, W.B. (2017), "Unified solution to drained expansion of a spherical cavity in clay and sand", *Int. J. Geomech.*, **17**(8), 04017028. https://doi.org/10.1061/(ASCE)GM.1943-5622.0000909.

Li, L., Xiang, Z.C., Zou, J.F. and Wang, F. (2019), "An improved model of compaction grouting considering three-dimensional shearing failure and its engineering application", *Geomech. Eng.*, **19**(3), 217-227. https://doi.org/10.12989/gae.2019.19.3.217.

Liang, F.Y., Liang, X., Zhang, H. and Wang, C. (2020), "Seismic response from centrifuge model tests of a scoured bridge with a pile-group foundation", *J. Bridge Eng.*, **25**(8), 04020054. https://doi.org/10.1061/(ASCE)BE.1943-5592.0001594.

Liang, Q.G., Li, J., Wu, X.Y. and Zhou, A.N. (2016), "Anisotropy of Q2 loess in the Baijiapo Tunnel on the Lanyu Railway, China", *B. Eng. Geol. Environ.*, **75**(1), 109-124. https://doi.org/10.1007/s10064-015-0723-z.

Liu, F., Yi, J.T., Cheng, P. and Yao, K. (2020), "Numerical simulation of set-up around shaft of XCC pile in clay", *Geomech. Eng.*, **21**(5), 489-501. https://doi.org/10.12989/gae.2020.21.5.489.

Lukic, D.C., Prokic, A.D. and Brcic, S.V. (2014), "Stress state around cylindrical cavities in transversally isotropic rock mass", *Geomech. Eng.*, **6**(3), 213-233. https://doi.org/gae.2014.6.3.213.

Mayne, P.W. (1991), "Determination of OCR in clays by piezocone tests using cavity expansion and critical state concepts", *Soils Found.*, **31**(2), 65-76. https://doi.org/10.3208/sandf1972.31.2_65.

Pournaghiazar, M., Russell, A.R. and Khalili, N. (2012), "Linking cone penetration resistances measuredin calibration chambers and the field", *Geotech. Lett.*, **2**, 26-35. https://doi.org/10.1680/geolett.11.00040.

Randolph, M.F. (2003), "Science and empiricism in pile foundation design", *Géotechnique*, **53**(10), 847-875. https://doi.org/10.1680/geot.53.10.847.37518.

Rezania, M., Nezhad, M.M., Zanganeh, H., Castro, J. and Sivasithamparam, N. (2017), "Modeling pile setup in natural clay deposit considering soil anisotropy, structure, and creep effects: case study", *Int. J. Geomech.*, **17**(3), 1-13. https://doi.org/10.1061/(ASCE)GM.1943-5622.0000774.

Russell, A.R. and Khalili, N. (2006), "On the problem of cavity expansion in unsaturated soils", *Comput. Mech.*, **37**(4), 311-330. https://doi.org/10.1007/s00466-005-0672-7.

Salgado, R., Mitchell, J.K. and Jamiolkowski, M. (1997), "Cavity expansion and penetration resistance in sand", *J. Geotech. Geoenviron. Eng.*, **123**(4), 344-354. https://doi.org/10.1061/(ASCE)1090-0241(1997)123:4(344).

Sheng, D., Fredlund, D.G. and Gens, A. (2008), "A new modelling approach for unsaturated soils using independent stress variables", *Can. Geotech. J.*, **45**(4), 511-534. https:// doi.org/10.1139/T07-112.

Silvestri, V. and Abou-Samra, G. (2012), "Analytical solution for undrained plane strain expansion of a cylindrical cavity in modified cam clay", *Geomech. Eng.*, **4**(1), 19-37. https://doi.org/10.12989/gae.2012.4.1.019.

Sivasithamparam, N. and Castro, J. (2018), "Undrained expansion of a cylindrical cavity in clays with fabric anisotropy: Theoretical solution", *Acta. Geotech.*, **13**(3), 729-746. https://doi.org/10.1007/s11440-017-0587-4.

Sivasithamparam, N. and Castro, J. (2020), "Undrained cylindrical cavity expansion in clays with fabric anisotropy and structure: Theoretical solution", *Comput. Geotech.*, **120**. https://doi.org/10.1016/j.compgeo.2019.103386.

Sun, D.A., Sheng, D., Li. X. and Scott W.S. (2008), "Elastoplastic prediction of hydro-mechanical behaviour of unsaturated soils under undrained conditions", *Comput. Geotech.*, **35**(6), 845-852. https://doi.org/10.1016/j.compgeo.2008.08.002.

Vesic, A.C. (1972), "Expansion of cavities in infinite soil mass", *J. Soil Mech. Found. Div.*, **98**, 265-290.

Vrakas, A. and Anagnostou, G. (2015), "Finite strain elastoplastic solutions for the undrained ground response curve in tunneling", *Int. J. Numer. Anal. Mech. Geomech.*, **39**(7), 738-761. https://doi.org/10.1002/nag.2335.

Wang, Y., Li, L., Li, J.P. and Sun, D.A. (2020), "Jet-grouting in ground improvement and rotary grouting pile installation: Theoretical analysis", *Geomech. Eng.*, **21**(3), 279-288. https://doi.org/10.12989/gae.2020.21.3.279.

Wheeler, S.J., Sharma, R.S. and Buisson, M.S.R. (2003), "Coupling of hydraulic hysteresis and stress-strain behavior in unsaturated soils", *Géotechnique,* **53**(1), 41-54. https://doi.org/10.1680/geot.2003.53.1.41.

Yang, C.Y., Chen, H.H., and Li, J.P. (2020). "Drained cylindrical cavity expansion analysis in anisotropic soils considering 3D strength" *Géotech. Lett.*, **10**, 346-352. https://doi.org/10.1680/jgele.19.00043.

Yang, C.Y., Chen, H.H., Li, J.P. and Li, L. (2021b), "Undrained spherical cavity expansion in unsaturated soils: Semi-analytical solution coupling hydraulic and mechanical behaviors", *Int. J. Geomech.*, **21**(6), 04021070. https://doi.org/10.1061/(ASCE)GM.1943-5622.0002028.

Yang, C.Y., Li, J.P., Li, L. and Sun D.A. (2021a), "Expansion responses of a cylindrical cavity in overconsolidated unsaturated soils: A semi-analytical elastoplastic solution", *Comput. Geotech.*, **130**, 103922. https://doi.org/10.1016/j.compgeo.2020.103922.

Yang, H. and Russell, A.R. (2015), "Cavity expansion in unsaturated soils exhibiting hydraulic hysteresis considering

three drainage conditions", *Int. J. Numer. Anal. Met.*, **39**(18), 1975-2016. https://doi.org/10.1002/nag.2379.

Yu, H.S. and Houlsby, G.T. (1991), "Finite cavity expansion in dilatant soils: Loading analysis", *Géotechnique*, **41**(2), 173-183. https://doi.org/10.1680/geot.1991.41.2.173.

Zhang, L.Y., Cao, P. and Radha, K.C. (2010), "Evaluation of rock strength criteria for wellbore stability analysis", *Int. J. Rock Mech. Min. Sci.*, **47**(8), 1304-1316. https://doi.org/10.1016/j.ijrmms.2010.09.001.

Zhou, X.Y., Xu, Y.S., Sun, D.A., Tan, Y.Z. and Xu, Y.F. (2021), "Three-dimensional thermal-hydraulic coupled analysis in the nuclear waste repository", *Ann. Nucl. Energy*, **151**, 107866. https://doi.org/10.1016/j.anucene.2020.107866.

Zou, J.F. and Xia, M.Y. (2017), "A new approach for the cylindrical cavity expansion problem incorporating deformation dependent of intermediate principal stress", *Geomech. Eng.*, **12**(3), 347-360. https://doi.org/10.12989/gae.2017.12.3.347.

Zou, J.F., Yang, T., Ling, W., Guo, W.J. and Huang, F.L. (2019), "A numerical stepwise approach for cavity expansion problem in strain-softening rock or soil mass", *Geomech. Eng.*, **18**(3), 225-234. https://doi.org/10.12989/gae.2019.18.3.225.

GC

Appendix

According to the plastic consistency condition, the total differential of the yield function f can be given as:

$$\mathrm{D}f = \frac{\partial f}{\partial p'}\mathrm{D}p' + \frac{\partial f}{\partial q}\mathrm{D}q + \frac{\partial f}{\partial p'_{\mathrm{y}}}\mathrm{D}p'_{\mathrm{y}} = 0 \tag{A1}$$

Due to p'_y is function of s and p'_{0y}, Eq. (A1) can be further expressed as:

$$\mathrm{D}f = \frac{\partial f}{\partial p'}\mathrm{D}p' + \frac{\partial f}{\partial q}\mathrm{D}q + \frac{\partial f}{\partial p'_{\mathrm{y}}}\left(\frac{\partial p'_{\mathrm{y}}}{\partial s}\mathrm{D}s + \frac{\partial p'_{\mathrm{y}}}{\partial p'_{0\mathrm{y}}}\mathrm{D}p'_{0\mathrm{y}}\right) = 0 \tag{A2}$$

The increment of p'_{0y} can be related to the increment of plastic volume strain $\mathrm{D}\varepsilon_{\mathrm{v}}^{\mathrm{p}}$ based on the hardening law as:

$$\mathrm{D}p'_{0\mathrm{y}} = p'_{0\mathrm{y}}\frac{v}{\lambda(0)-\kappa}\mathrm{D}\varepsilon_{\mathrm{v}}^{\mathrm{p}} \tag{A3}$$

Based on the associated flow law, Eq. (A3) can be further expressed:

$$\mathrm{D}p'_{0\mathrm{y}} = p'_{0\mathrm{y}}\frac{v}{\lambda(0)-\kappa}\Lambda\frac{\partial f}{\partial p'} \tag{A3}$$

Substituting Eq. (A3) into Eq. (A2) can give the expression of scalar multiplier Λ as:

$$\begin{aligned}\Lambda &= -\frac{\frac{\partial f}{\partial p'}\mathrm{D}p' + \frac{\partial f}{\partial q}\mathrm{D}q + \frac{\partial f}{\partial p'_{\mathrm{y}}}\frac{\partial p'_{\mathrm{y}}}{\partial s}\mathrm{D}s}{\frac{\partial f}{\partial p'_{\mathrm{y}}}\frac{\partial p'_{\mathrm{y}}}{\partial p'_{0\mathrm{y}}}p'_{0\mathrm{y}}\frac{v}{\lambda(0)-\kappa}\frac{\partial f}{\partial p'}} \\ &= -\frac{\frac{\partial f}{\partial \sigma'_{ij}}\mathrm{D}\sigma'_{ij} + \frac{\partial f}{\partial p'_{\mathrm{y}}}\frac{\partial p'_{\mathrm{y}}}{\partial s}\mathrm{D}s}{\frac{\partial f}{\partial p'_{\mathrm{y}}}\frac{\partial p'_{\mathrm{y}}}{\partial p'_{0\mathrm{y}}}p'_{0\mathrm{y}}\frac{v}{\lambda(0)-\kappa}\frac{\partial f}{\partial p'}}\end{aligned} \tag{A4}$$

where

$$\frac{\partial f}{\partial p'} = (M^2-\eta^2)p' \tag{A5}$$

$$\frac{\partial f}{\partial q} = 2q \tag{A6}$$

$$\frac{\partial f}{\partial p'_{\mathrm{y}}} = -M^2p' \tag{A7}$$

$$\frac{\partial p'_{\mathrm{y}}}{\partial s} = \frac{\lambda(0)[\lambda(0)-\kappa](M^2+\eta^2)p'c(1-b)e^{-cs}}{M^2[\lambda(s)-\kappa]^2}\ln\left(\frac{p'_{0\mathrm{y}}}{p'_{\mathrm{n}}}\right) \tag{A8}$$

$$\frac{\partial p'_{\mathrm{y}}}{\partial p'_{0\mathrm{y}}} = \frac{\lambda(0)-\kappa}{\lambda(s)-\kappa}\left(\frac{p'_{0\mathrm{y}}}{p'_{\mathrm{n}}}\right)^{\frac{\lambda(0)-\lambda(s)}{\lambda(s)-\kappa}} \tag{A9}$$

$$\mathrm{D}p' = \frac{1}{3}\delta_{ij}\mathrm{D}\sigma'_{ij} \tag{A10}$$

$$\mathrm{D}q = \frac{3\left(\sigma'_{ij}-p'\delta_{ij}\right)}{2q}\mathrm{D}\sigma'_{ij} \tag{A11}$$

$$\eta = \frac{q}{p'} \tag{A12}$$